

Real-Time Vertical Path Planning Using Model Predictive Control for an Autonomous Marine Current Turbine

Arezoo Hasankhani¹, Yufei Tang¹, Yu Huang¹, and James VanZwieten²

Abstract—This paper presents a predictive approach to address real-time vertical path planning for a marine current turbine (MCT) treated as an autonomous underwater vehicle (AUV), where the path control goal is to maximize the total harvested ocean current energy. The real-time path planning is formulated as a sequence of optimization problems over a prediction horizon with respect to the autonomous MCT model and underwater environment model. The ocean current velocity is modeled through a spatiotemporal neural network (STNN) trained using field-collected acoustic Doppler current profiler (ADCP) data. Model predictive control (MPC)-based approach is proposed to solve the optimizations, where the proposed approach takes advantage of fast discrete path planning (i.e., path planning in a gridded ocean environment) to seek the initial solution, as well as continuous path planning to improve the initial solution in a continuous ocean environment. Results demonstrate that the proposed reinforced continuous path planning algorithm can find a better solution (i.e., optimal path) than independent continuous path planning.

I. INTRODUCTION

Marine hydrokinetic (MHK) turbines, including marine current turbines (MCT) and waver energy converters (WECs) that are being used to harness renewable power from puissant oceanic resources, have recently gained significant attention from academia and industry. An autonomous MCT system, similar to an autonomous underwater vehicle (AUV), is able to navigate itself without human intervention [1]. This level of autonomy necessitates precise path planning, facing challenges of the nonlinear and complex MCT system, as well as operation in a spatiotemporal uncertain underwater environment [2]. Path planning can pursue different goals, such as minimizing travel time [3], minimizing path length [4], or minimizing energy consumption [5]. Here, the primary goal of an autonomous MCT is to find the path (i.e., operation depth) that maximizes the harnessed power from the ocean current since the ocean current speed is depth-dependent and time-varying.

To cope with the path planning of AUVs, heavy research has been done in the literature relying on discrete or continuous representations from the underwater environment. For example, graph search methods, including Dijkstra's algorithm [6], A* algorithm [7], and D* algorithm [8], are classical path planning approaches to address the graph

This work was supported by the National Science Foundation under Grant Nos. ECCS-1809164, CMMI-2145571, & OAC-2017597 and the U.S. Department of Energy under Grant No. DE-EE0008955.

¹Department of Electrical Engineering and Computer Science, Florida Atlantic University, Boca Raton, FL 33431, USA. {ahasankhani2019, tangy, yhwang2018}@fau.edu.

²Department of Civil, Environmental and Geomatics Engineering, Florida Atlantic University, Boca Raton, FL 33431, USA. jvanzwi@fau.edu.

constructed by the discretized environment, which are fast but suffering from lower precision due to discretization and computational complexity in the high-dimensional environment. On the other hand, popular planning approaches for continuous environment rely on heuristic algorithms [9], learning-based methods [10], and predictive algorithms [11]. Predictive methodologies, especially model predictive control (MPC), have shown promising performance in real-time path planning for different autonomous vehicles operating in dynamic underwater environment [12].

Traditional path planning methods are not devoted to the environment prone to an uncertain ocean current with turbulence and shear; thus, there is a need for a dedicated predictive method to take care of ocean current prediction. MPC solves the path planning as a sequence of problems over a prediction horizon considering the sequential state updates in the environment and autonomous system. Here, one of the major tasks is to formulate the path planning as an optimization problem taking into account the AUV's dynamics. Note that the MPC approach has been commonly applied to address the path tracking problem to minimize the tracking error subject to the system dynamics [13]–[16]. However, very little research has been done toward addressing the AUV path planning using the MPC. For example, an MPC-based real-time navigation optimization has been proposed for the AUVs to minimize the squared distance from the target state [17]; a coupled sample-based path planning with MPC has been used to simultaneously seek the optimal actuators and path for the AUV [18]. In a similar study [19], an energy-harvesting AUV has been investigated to find the optimal path to maximize the total energy, yet lacking a detailed system model. There is a need to develop an efficient path planning algorithm that considers both spatiotemporal uncertain underwater environments and detailed AUV dynamics.

The main contribution of this paper is to propose a reinforced MPC approach to address the spatiotemporal path planning for an autonomous MCT (initially modeled in [20]). First, the ocean current velocity is modeled through a spatiotemporal neural network (STNN) trained using real velocity data recorded in the Gulf Stream. Then, real-time vertical path planning based on MPC is presented for the autonomous MCT, which seeks to maximize the harvested power. The optimal vertical path is found according to the MCT movement constraints and the predictions of the ocean current, where the path planning problem is first solved under discrete (gridded) representation from the underwater environment to compute an initial solution, which is then

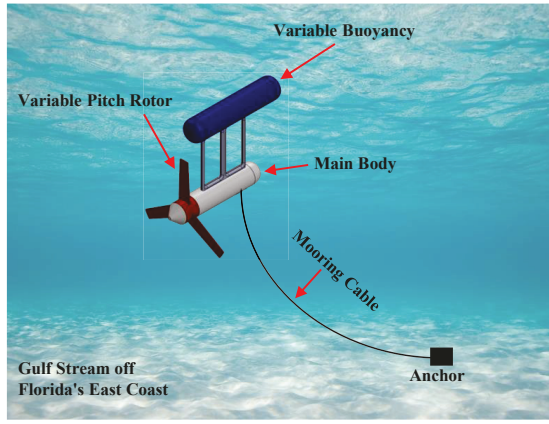


Fig. 1. Schematic diagram of the autonomous marine current turbine.

given as an initial guess to the real-time path planning defined in a continuous environment.

The remainder of this paper is organized as follows. Section II introduces the autonomous MCT system model. Section III describes the algorithm to model the ocean current, the real-time path planning problem, and the proposed problem solution. The simulation results and discussion are presented in Section IV. Finally, conclusions and future works are provided in Section V.

II. AUTONOMOUS MARINE CURRENT TURBINE MODELING

This paper focuses on an energy-harvesting AUV, entitled autonomous MCT, which is designed to operate in the Gulf Stream off Florida's East Coast [20]. It is noteworthy to mention that the MCT system is recently co-designed to couple the physical design and path control [21], which is beyond the scope of the current study. The MCT system has a rated power of 700 kW, following the prototypes presented by IHI Corp. [22], and the university of Naples [23], but equipped with a single variable pitch rotor, one variable buoyancy chamber placing two variable buoyancy tanks, main pressure vessel (main body), and a 607 m mooring cable to tether the MCT to the ocean floor (Fig. 1). The investigated autonomous MCT is designed to operate near the equilibrium depth of 50 m in an ocean current speed of 1.6 m/s with half-filled variable buoyancy tanks.

The autonomous MCT is primarily controlled in its vertical movement through two actuators, i.e., variable buoyancy fill fractions denoted by B_f and B_a ; note that there exists another actuator in the MCT, which is electromechanical torque T_{em} (not affecting the vertical movement). The autonomous MCT system is then controlled through its actuators $[B_f B_a T_{em}]$. The MCT system is modeled with 14 states: the linear body position $[x y z]$, the angular body position $[\phi_b \theta \psi]$, the linear body velocity $[u v w]$, the angular body velocity $[p_b q r]$, the rotation angle and velocity of the rotor $[\phi_r p_r]$. The MCT system is represented by 7 degrees-of-freedom (DOF), consisting of 6 DOF of the main body and 1 DOF of the rotor's rotation about the x-axis. The equations of motion for this 7 DOF are formulated in (1) and (2):

$$\dot{p}_r = \frac{M_{x_r} - \tau_{em} - qr(I_{z_r} - I_{y_r})}{I_{x_r}} \quad (2)$$

where, $f_{(\cdot)}$ and $M_{(\cdot)}$ denote the force and moment about (\cdot) ; $m_{(\cdot)}$ and $I_{(\cdot)}$ are the mass and the moment of inertia, respectively.

To reduce the computational burden of the path planning using the full complex nonlinear dynamic model of the autonomous MCT, we will approximate the movement about z-direction (vertical movement) with a linear model as the most favorable state for the vertical path planning problem. The whole procedure of acquiring the linear model of MCT vertical movement and its justification with the nonlinear model was presented in the authors' previous work [24], which is briefly reviewed here.

Linear Model of MCT Vertical Movement: The nonlinear model of the MCT is approximated to leverage a linear equation for the vertical movement based on B_f and B_a . To place the autonomous MCT at a certain operating depth, the system should be able to vertically move to that certain depth and hold the depth by resisting the velocity changes. The first part (changing the depth) is characterized with Δz , and the latter is denoted by Δv , thereby formulating the changes in the fill fraction by Δz and Δv as follows:

$$\Delta B = \beta_1 \Delta v + \beta_2 \Delta z \quad (3)$$

where $\beta_1 = \frac{dB}{dz} \frac{dz}{dv}$ and $\beta_2 = \frac{dB}{dz}$ are the constant coefficients calculated according to the nonlinear model of the MCT.

The total harnessed power from the autonomous MCT is formulated as a closed-form equation using a similar manner to finding a linear vertical movement from the nonlinear model [24], as shown in (4a)-(4d):

$$P_{net} = P_{MCT} - P_{HD} - P_{CD} \quad (4a)$$

$$P_{MCT} = \min\left(\frac{1}{2} \rho A v^3 c_p, P_n\right) \quad (4b)$$

$$P_{HD} = \begin{cases} 0, & \Delta v < 0 \\ \frac{\beta_1}{T_s} \Delta v, & \Delta v > 0 \end{cases} \quad (4c)$$

$$P_{CD} = \begin{cases} 0, & \Delta z > 0 \\ \frac{\beta_2}{T_s} \Delta z, & \Delta z < 0 \end{cases} \quad (4d)$$

where ρ is the water density, A denotes the rotor area, v is the ocean current velocity, c_p is the power coefficient [25], P_n is the MCT nominal power, and T_s is the sampling time.

III. REAL-TIME PATH PLANING USING MODEL PREDICTIVE CONTROL

In this section, the overall real-time path planning problem is formulated for the MCT. We first present the STNN for modeling ocean current velocity, followed by ocean environment representation, and finally discuss our proposed approach for real-time path planning.

$$\begin{bmatrix} \ddot{x} \\ \ddot{y} \\ \ddot{z} \\ \dot{\Phi}_b \\ \dot{\theta} \\ \dot{\Psi} \end{bmatrix} = \begin{bmatrix} m & 0 & 0 & 0 & m^b z_G^b & 0 \\ 0 & m & 0 & -m^b z_G^b & 0 & mx_G \\ 0 & 0 & m & 0 & -mx_G & 0 \\ 0 & -m^b z_G^b & 0 & I_x^b & 0 & -I_{xz}^b \\ m^b z_G^b & 0 & -mx_G & 0 & I_y & 0 \\ 0 & mx_G & 0 & -I_{xz}^b & 0 & I_z \end{bmatrix}^{-1} \begin{bmatrix} F_x + m(vr - wq) + mx_G(q^2 + r^2) - m^b z_G^b p^b r \\ F_y - mur + w(m^b p^b + m^r p^r) - m^b z_G^b qr \\ -m^b x_G^b qp^b - m^r x_G^b qp^r \\ F_z + muq - v(m^b p^b + m^r p^r) + m^b z_G^b(p^{b2} + q^2) \\ -m^b x_G^b rp^b - m^r x_G^b rp^r \\ M_x + M_x^s - qr(I_z^b - I_y^b) + I_{xz}^b p^b q \\ -m^b z_G^b(wp^b - ur) \\ M_y - rp^b(I_x^b - I_z^b) - rp^r(I_x^r - I_z^r) - I_{xz}^b(p^{b2} - r^2) \\ + m^b z_G^b(vr - wq) - mx_G uq + m^b x_G^b vp^b + m^r x_G^b vp^r \\ M_z - qp^b(I_y^b - I_x^b) - qp^r(I_y^r - I_x^r) - I_{xz}^b rq \\ -mx_G u r + m^b x_G^b wp^b + m^r x_G^b wp^r \end{bmatrix} \quad (1)$$

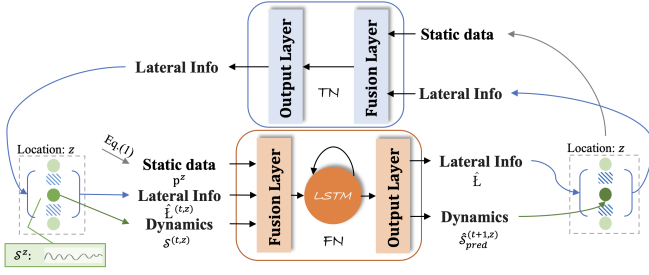


Fig. 2. Proposed STNN for ocean current velocity modeling. The green node denotes a center node located at depth z , and faded green nodes are its neighbors. Three types of information are used to characterize each node: (1) Dynamics $S^{(t,z)}$: an embedding vector that represents status of node at time t ; (2) Static Info $\tilde{\mathbf{p}}^z$: an embedding vector that represents node location; and (3) Lateral Info $\mathbf{L}^{(t,z)}$: an embedding vector (dashed dot-square set) capturing interaction (lateral info) between each node and its neighbors.

A. Spatiotemporal Neural Network for Ocean Current Velocity Modeling

To deal with a predictive approach for addressing real-time path planning, it is necessary to build a model of the ocean current velocity for forecasting the future velocities. Here, a spatiotemporal variable nature of the ocean velocity data complicates the model. The ocean current along with the depth exhibit heterogeneous properties, so we adopt the simplified version of the spatiotemporal neural network (STNN) proposed in [26] to forecast the ocean current.

The STNN is a bi-network architecture, as shown in Fig. 2, consisting of a forecasting network (FN) and a transition network (TN). FN receives (i) dynamic data, which is evolutionary predicted and changed over time; (ii) static information, which stays constant and characterizes the location of each FN; and (iii) lateral information from neighbors. The output of each FN includes predicted dynamics and additional lateral information that will be interacted with its neighbors. Such interactions are conducted through a TN with two-stacked linear layers, which aims to model the location-sensitive transitions between adjacent FNs and thus enabling local spatial-dependent information propagation.

To enable the model to leverage localization information, information about the absolute position of each depth through positional encoding [26] is needed. In particular, let z be the desired position along depth, $\tilde{\mathbf{p}}^z \in \mathbb{R}^D$ be its corresponding

encoding, D be the encoding dimension, and $d = [1, \dots, D]$ be the element index in the encoded vector. Then, the encoding scheme \mathcal{E} is defined as:

$$\tilde{\mathbf{p}}^z = \mathcal{E}(z) \in \mathbb{R}^D; \mathcal{E}(\ast)^d = \begin{cases} \sin(\ast \cdot \omega_k) & \text{if } d = 2k \\ \cos(\ast \cdot \omega_k) & \text{if } d = 2k + 1 \end{cases} \quad (5)$$

where $\omega_k = \frac{1}{10,000^{2k/D}}$, $k \in \mathbb{N}_{\leq \lfloor \frac{D}{2} \rfloor}$. The wavelengths form a geometric progression from 2π to $10000 \cdot 2\pi$. Since the positional embedding is a vector that contains pairs of sines and cosines for each decreasing frequency along the vector dimension, it allows the model to easily learn the relative positions of the grid nodes. As illustrated in Fig. 2, the FN and TN are executed in space simultaneously. At each time t , the TN first encodes the node's lateral info \mathbf{L} and static info $\tilde{\mathbf{p}}$ as follows:

$$\mathbf{L}_{enc}^{(t,z)} = \text{Relu}([\tilde{\mathbf{p}}^z, \mathbf{L}^{(t,z)}]W_T^T + b_T) \quad (6)$$

where $\theta_T = [W_T, b_T]$ denote the weights and bias of TN. $\mathbf{L}^{(t,z)}$ is a vector used to characterize interaction between a node at z and its neighbors. \mathbf{L} is only aggregated over the nearest neighbours. It is initialized as zero and continuously updated by (11) when $t > 0$. Then, FN encodes each view (i.e., static $\tilde{\mathbf{p}}$, dynamics S , and encoded \mathbf{L}_{enc} of each node) using a fusion layer as:

$$f^{(t,z)} = [\tilde{\mathbf{p}}^z, S^{(t,z)}, \mathbf{L}_{enc}^{(t,z)}]W_{fusion}^T + b_{fusion} \quad (7)$$

These features, $f^{(t,z)} \in \mathbb{R}^{d_{fz}}$, are then fed into a long short-term memory (LSTM) to model the node-specific interactions over time. The update mechanism of the LSTM cell is defined as:

$$[I^{(t)}; F^{(t)}; \tilde{C}^{(t)}; O^{(t)}] = \sigma(W \cdot f^{(t,z)} + T \cdot h^{(t-1)}) \quad (8)$$

$$C^{(t)} = \tilde{C}^{(t)} \circ I^{(t)} \quad (9)$$

$$h^{(t)} = O^{(t)} \circ C^{(t)} \quad (10)$$

where $\sigma(\cdot)$ applies sigmoid on the input gate $I^{(t)}$, forget gate $F^{(t)}$, and output gate $O^{(t)}$, as well as $\tanh(\cdot)$ on memory cell $\tilde{C}^{(t)}$. The parameters are characterized by $W \in \mathbb{R}^{d_{fz} \times d_{hz}}$ and $T \in \mathbb{R}^{d_{hz} \times d_{hz}}$, where d_{hz} is the output dimension. A cell updates its hidden states $h^{(t)}$ based on the previous step $h^{(t-1)}$ and the current input $f^{(t,z)}$. An output layer is stacked at the

TABLE I

COMPARATIVE STUDY OF A SINGLE STEP PREDICTION PERFORMANCE

Model	MSE	RMSE	MAE
Conv-tt-LSTM [27]	0.023	0.079	0.055
Transformer [28]	0.027	0.107	0.077
Proposed STNN	0.022	0.076	0.053

end of FN to transform the LSTM output into the expected dynamic prediction and the additional lateral information:

$$\left[\hat{\mathbf{S}}^{(t,z)}; \hat{\mathbf{L}}^{(t,z)} \right] = \text{Relu}(W_{out} \cdot f^{(t,z)} + b_{out}) \quad (11)$$

where $\hat{\mathbf{S}}^{(t,z)}$ denotes the prediction of the node dynamics at time step t . The learnable parameters are characterized by $W^{(t)} \in \mathbb{R}^{d_{fz} \times d_{yz}}$ and $b_{out} \in \mathbb{R}^{d_{yz}}$ assuming d_{yz} denotes the total dimension of the dynamic and the lateral outputs.

The proposed STNN is trained using real velocity data, and once the offline training is done, the network weights are fixed, and the model is applied online to forecast the ocean current velocity. The single step performance of STNN is compared with two other algorithms, and the comparative results are shown in TABLE I.

B. Discrete or Continuous Environment Representation

The environment is represented in 1D (z-direction) since the autonomous MCT can primarily move in the vertical direction. In reality, there are two ways to implement this vertical path planning: a discrete manner that the turbine can only move to several discrete depths or a continuous manner that the turbine can move to any depth. In a gridded environment, the discretized operating depth (waypoint) and history of recorded ocean current velocity are fully known. Note that the operating depth is discretized every 5 m within the allowable depth range (21 waypoints), and the prediction horizon is N sampling time (i.e., predicted by the aforementioned STNN); the environment size is then $21 \times N$. While in the continuous environment, the autonomous MCT can continuously move to any feasible depth.

C. Path Planning Problem Formulation

The real-time path planning for autonomous MCT is formulated as a nonlinear optimization problem presented in (12a)-(12f), as follows:

$$\mathbf{z}^*(k) = \arg \min_{\mathbf{z}(k)} \sum_{t=k}^{k+N-1} -E(P_{\text{net}}(z(t|k), v_*(t|k), z(t|k))) \quad (12a)$$

subject to

$$v_* = \text{STNN}(t, z) \quad (12b)$$

$$B_{(\cdot)}(t+1|k) = B_{(\cdot)}(t|k) + \beta_1 \Delta v + \beta_2 \Delta z \quad (12c)$$

$$B_{(\cdot)}^{\min} \leq B_{(\cdot)} \leq B_{(\cdot)}^{\max} \quad (12d)$$

$$\dot{B}_{(\cdot)} \leq \dot{B}_{(\cdot)}^{\max} \quad (12e)$$

$$z^{\min} \leq z(t|k) \leq z^{\max} \quad (12f)$$

To solve this optimization problem, an MPC approach is applied that solves a finite sequence of path planning problems over a prediction horizon N . Let $\mathbf{z}(k) \triangleq$

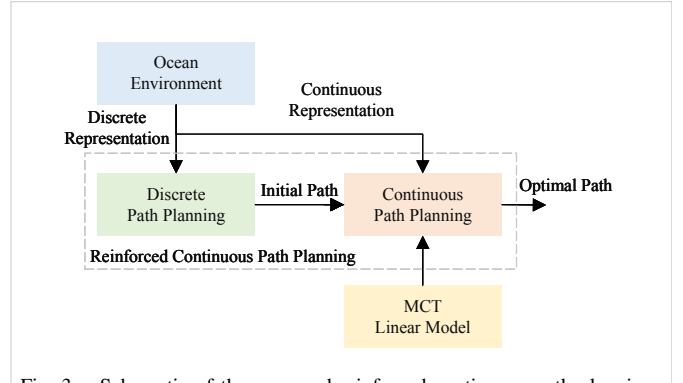


Fig. 3.— Schematic of the proposed reinforced continuous path planning.

$[z(k|k), \dots, z(k+N-1|p)]^T$ as an operating depth sequence, $\mathbf{z}^*(k) \triangleq [z^*(k|k), \dots, z^*(k+N-1|k)]$ as an optimal operating depth sequence. Constraint (12b) represents the predicted velocity v_* using a spatiotemporal neural network; constraint (12c) deals with the linear model of vertical MCT movement; Other constraints formulate the fill fraction limits (12d), fill fraction rate (12e), and operating depth limit (12f). Note that the investigated real-time path planning is a nonlinear and non-convex problem due to constraint (12b) enforcing the ocean current velocity forecasting model.

D. Proposed Solution for Path Planning Optimization

The proposed approach entitled “reinforced continuous path planning” includes two sub-modules: (i) discrete path planning; and (ii) continuous path planning (Fig. 3). The approach will solve the path planning problem based on an initial solution provided by solving the optimization problem in a discrete gridded environment (discrete path planning), where the discrete MPC path planning problem is relaxed by removing the linear MCT movement constraint. This initial solution is then given to the real-time path planning (continuous path planning) defined in a continuous operating environment that is presented in Section III-B. Note that the optima is improved by finding a desirable initial solution from a so-called discrete path planning.

Discrete path planning considering a discrete representation of ocean environment: The discrete path planning is responsible for finding an initial solution for the MPC optimization problem, but the precision is limited by the discrete grid size. To solve the discrete MPC optimization, dynamic programming by forward recursion is used, where the global optima is found in the discrete environment resolution.

Real-time path planning considering a continuous ocean environment: The real-time path planning takes care of finding an optimal path in a continuous underwater environment, which improves the initial solution received from the discrete path planning. To solve this nonlinear optimization problem, the “fmincon” solver of the Matlab optimization toolbox is used.

IV. EXPERIMENTAL RESULTS

A. Simulation Setup

The proposed approach is evaluated for an autonomous MCT presented in [20]. The MCT parameters are $\rho =$

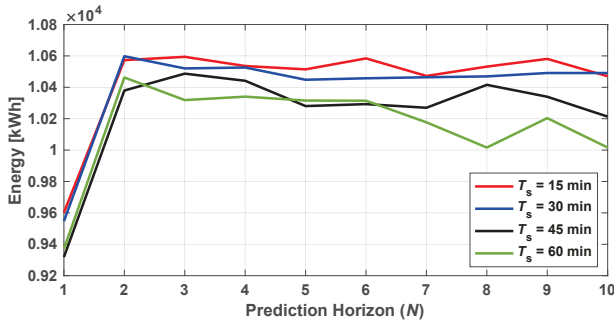


Fig. 4. Comparing cumulative energy obtained by an reinforced continuous path planning over a 24-hour of the simulation under different sampling time (T_s) and prediction horizon (N); the best cumulative energy is obtained under $T_s = 30$ min and $N = 2$.

1030 kg/m^3 , $A = 100\pi$, $c_p = 0.41$, $\beta_1 = 9.113$, and $\beta_2 = -0.0365$. To enable the spatiotemporal neural network, a sample ocean current velocity data is used, which is recorded by a 75 kHz acoustic Doppler current profiler (ADCP) in the Gulf Stream. The other parameters in the MPC problem include $B_{(\cdot)}^{\min} = 0$, $B_{(\cdot)}^{\max} = 1$, $\dot{B}_{(\cdot)}^{\max} = 7.45 \times 10^{-4}$, $z_{\min} = 50$, and $z_{\max} = 150$. All simulations were run in Matlab on a CPU @2.3 GHz with 32 Gb of RAM. The following scenarios are simulated and compared:

Discrete Path Planning: The path planning is addressed in a gridded discrete environment as described in Section III-B, where the spatiotemporal ocean environment is modeled with a $21 \times N$ grid.

Continuous Path Planning: The optimal vertical path is planned for the autonomous MCT operating in the continuous ocean environment. A sequence of optimal depth is obtained over a horizon of length N .

Reinforced Continuous Path Planning: The initial optimal path is found by the discrete path planning, which is then given to the continuous path planning to improve the final solution taking advantage of both discrete and continuous representations from the ocean environment.

B. Results and Discussions

To justify the prediction horizon and sampling time for the MPC problem, a comparative analysis is performed to seek the cumulative energy obtained over different sampling times and prediction horizons, as shown in Fig. 4. The best values obtained for these two parameters are $T_s = 30$ min and $N = 2$; the importance of a predictive methodology ($N > 1$) is also verified in this figure, where the results by a non-predictive approach ($N = 1$) are much smaller than the predictive approach. Hence, it is favorable to approach the real-time vertical path planning problem of the autonomous MCT through the MPC algorithm.

Fig. 5 depicts an optimal vertical path, velocity, power, and energy over a 100-hour of the simulation assuming $T_s = 30$ min and $N = 2$; these results are shown for (i) discrete MPC algorithm, (ii) continuous MPC algorithm, and (iii) reinforced continuous MPC algorithm. Note that the power shown in this figure implies an average power over a sampling time. The optimal depth for the discrete MPC

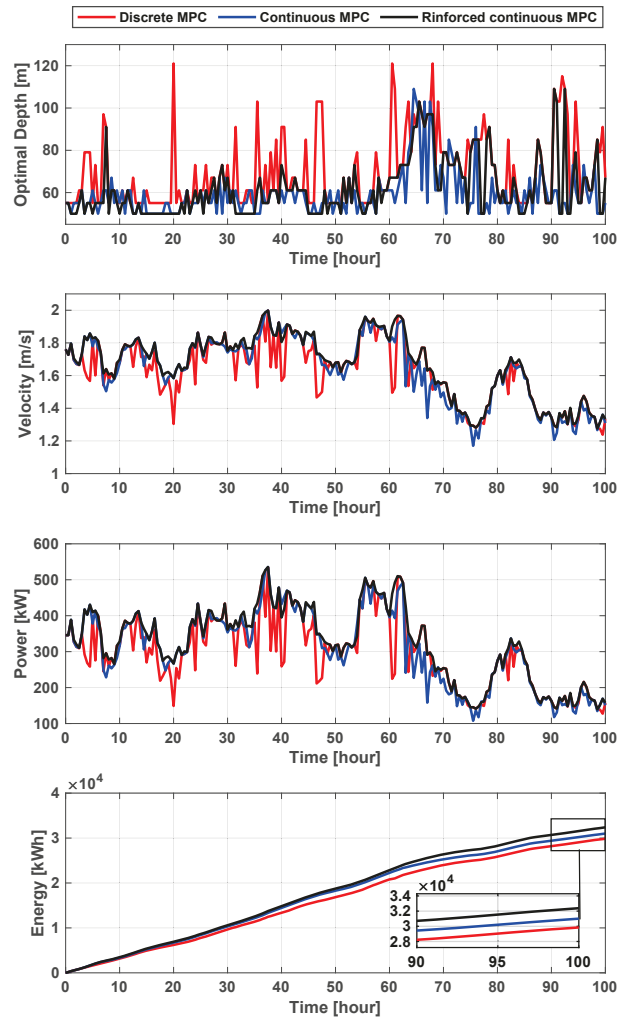


Fig. 5. Comparison of the optimal sequences determined by: (i) Discrete MPC algorithm; (ii) Continuous MPC algorithm; and (iii) Reinforced continuous MPC algorithm. In this figure, (a) optimal depth, (b) optimal velocity, (c) optimal power, and (d) optimal energy are shown.

yields more violations than allowed by the linear model of MCT due to relaxing the MPC problem by removing the movement model of MCT under the discrete algorithm. On the other hand, the optimal vertical path and velocity by two continuous approaches are much more similar than the discrete approach. It can be further seen that the reinforced continuous MPC surpasses the remaining methods in finding the optimal power. Note that the details for the control inputs and tracking controller results are given in [16]. The cumulative energy for the discrete MPC, the continuous MPC, and the reinforced continuous MPC are 29.848 MWh, 31.007 MWh, 32.386 MWh after a 100-hour operation. Although these values of energy production are close, still the reinforced continuous MPC shows the best performance. It should be noted that these values are obtained after a finite time of simulation, and this difference is intensified considering a real-time application.

The discrete path planning algorithm as a graph-based method is commonly criticized, prone to less precision limited to the discretization size, thereby enforcing the specific

length of movement at each time step. The spatial discretization size in the problem at hand seems precise enough to find an acceptable optimal path by taking a careful look at the cumulative energy. The computational complexity is an issue for discrete path planning in a large ocean environment. Hence, it is inevitable to use the continuous MPC, which follows the natural movement of the autonomous MCT. The nonlinear and non-convex nature of the path planning problem requires a longer time of convergence. To avoid trapping in the local optima and accelerating the convergence, the continuous path planning receives its initial value according to the optimal solution found through the discrete MPC.

V. CONCLUSIONS

Real-time vertical path planning using a reinforced continuous MPC was presented for an autonomous MCT. The proposed path planning problem combined the path planning under the discrete representation of the ocean environment (discrete path planning) with the continuous one. The initial path was provided by the discrete path planning, and the continuous path planning followed this initial solution, showing better performance in terms of finding the optimal path and maximum harvested power. Future works will focus on evaluating the robustness of the proposed approach and presenting a path planning of an array of autonomous MCTs.

REFERENCES

- [1] A. Hasankhani, Y. Tang, J. VanZwieten, and C. Sultan, "Comparison of deep reinforcement learning and model predictive control for real-time depth optimization of a lifting surface controlled ocean current turbine," in *2021 IEEE Conference on Control Technology and Applications (CTA)*. IEEE, 2021, pp. 301–308.
- [2] C. Shen, Y. Shi, and B. Buckham, "Integrated path planning and tracking control of an auv: A unified receding horizon optimization approach," *IEEE/ASME Transactions on Mechatronics*, vol. 22, no. 3, pp. 1163–1173, 2016.
- [3] M. Chyba, T. Haberkorn, R. Smith, and S. Choi, "Design and implementation of time efficient trajectories for autonomous underwater vehicles," *Ocean Engineering*, vol. 35, no. 1, pp. 63–76, 2008.
- [4] M. Ataei and A. Yousefi-Koma, "Three-dimensional optimal path planning for waypoint guidance of an autonomous underwater vehicle," *Robotics and Autonomous Systems*, vol. 67, pp. 23–32, 2015.
- [5] B. Garau, A. Alvarez, and G. Oliver, "Path planning of autonomous underwater vehicles in current fields with complex spatial variability: an a* approach," in *Proceedings of the 2005 IEEE international conference on robotics and automation*. IEEE, 2005, pp. 194–198.
- [6] E. W. Dijkstra *et al.*, "A note on two problems in connexion with graphs," *Numerische mathematik*, vol. 1, no. 1, pp. 269–271, 1959.
- [7] K. P. Carroll, S. R. McClaran, E. L. Nelson, D. M. Barnett, D. K. Friesen, and G. N. William, "Auv path planning: an a* approach to path planning with consideration of variable vehicle speeds and multiple, overlapping, time-dependent exclusion zones," in *Proceedings of the 1992 Symposium on Autonomous Underwater Vehicle Technology*. IEEE, 1992, pp. 79–84.
- [8] D. Ferguson and A. Stentz, "Using interpolation to improve path planning: The field d* algorithm," *Journal of Field Robotics*, vol. 23, no. 2, pp. 79–101, 2006.
- [9] M. P. Aghababa, M. H. Amrollahi, and M. Borjkhani, "Application of ga, pso, and aco algorithms to path planning of autonomous underwater vehicles," *Journal of Marine Science and Application*, vol. 11, no. 3, pp. 378–386, 2012.
- [10] Y. Sun, J. Cheng, G. Zhang, and H. Xu, "Mapless motion planning system for an autonomous underwater vehicle using policy gradient-based deep reinforcement learning," *Journal of Intelligent & Robotic Systems*, vol. 96, no. 3–4, pp. 591–601, 2019.
- [11] J. Ji, A. Khajepour, W. W. Melek, and Y. Huang, "Path planning and tracking for vehicle collision avoidance based on model predictive control with multiconstraints," *IEEE Transactions on Vehicular Technology*, vol. 66, no. 2, pp. 952–964, 2016.
- [12] C. Liu, S. Lee, S. Varnhagen, and H. E. Tseng, "Path planning for autonomous vehicles using model predictive control," in *2017 IEEE Intelligent Vehicles Symposium (IV)*. IEEE, 2017, pp. 174–179.
- [13] C. Shen, Y. Shi, and B. Buckham, "Trajectory tracking control of an autonomous underwater vehicle using lyapunov-based model predictive control," *IEEE Transactions on Industrial Electronics*, vol. 65, no. 7, pp. 5796–5805, 2017.
- [14] R. M. Saback, A. G. S. Conceicao, T. L. M. Santos, J. Albiez, and M. Reis, "Nonlinear model predictive control applied to an autonomous underwater vehicle," *IEEE Journal of Oceanic Engineering*, vol. 45, no. 3, pp. 799–812, 2019.
- [15] T. D. Ngo, C. Sultan, J. H. VanZwieten, and N. I. Xiros, "Constrained control of moored ocean current turbines with cyclic blade pitch variations," *IEEE Journal of Oceanic Engineering*, vol. 46, no. 2, pp. 594–610, 2020.
- [16] A. Hasankhani, E. B. Ondes, Y. Tang, C. Sultan, and J. VanZwieten, "Integrated path planning and tracking control of marine current turbine in uncertain ocean environments," in *2022 American Control Conference (ACC)*. IEEE, Accepted.
- [17] D. C. Fernández and G. A. Hollinger, "Model predictive control for underwater robots in ocean waves," *IEEE Robotics and Automation letters*, vol. 2, no. 1, pp. 88–95, 2016.
- [18] C. V. Caldwell, D. D. Dunlap, and E. G. Collins, "Motion planning for an autonomous underwater vehicle via sampling based model predictive control," in *OCEANS 2010 MTS/IEEE SEATTLE*. IEEE, 2010, pp. 1–6.
- [19] S. Bin-Karim, M. Muglia, and C. Vermillion, "Centralized position optimization of multiple agents in spatiotemporally-varying environment: a case study with relocatable energy-harvesting autonomous underwater vehicles in the gulf stream," in *2019 IEEE Conference on Control Technology and Applications (CTA)*. IEEE, 2019, pp. 264–269.
- [20] A. Hasankhani, J. VanZwieten, Y. Tang, B. Dunlap, A. De Luera, C. Sultan, and N. Xiros, "Modeling and numerical simulation of a buoyancy controlled ocean current turbine," *International Marine Energy Journal*, vol. 4, no. 2, pp. 47–58, 2021.
- [21] A. Hasankhani, Y. Tang, A. Snyder, J. VanZwieten, and W. Qiao, "Control co-design for buoyancy-controlled mhk turbine: A nested optimization of geometry and spatial-temporal path planning," *2022 IEEE Conference on Control Technology and Applications (CTA)*, Accepted.
- [22] T. Ueno, S. Nagaya, M. Shimizu, H. Saito, S. Murata, and N. Handa, "Development and demonstration test for floating type ocean current turbine system conducted in kuroshio current," in *2018 OCEANS-MTS/IEEE Kobe Techno-Oceans (OTO)*. IEEE, 2018, pp. 1–6.
- [23] D. Coiro, G. Troise, F. Scherillo, A. De Marco, G. Calise, and N. Bizzarrini, "Development, deployment and experimental test on the novel tethered system gem for tidal current energy exploitation," *Renewable Energy*, vol. 114, pp. 323–336, 2017.
- [24] A. Hasankhani, Y. Tang, J. VanZwieten, and C. Sultan, "Spatiotemporal optimization for vertical path planning of an ocean current turbine," *IEEE Transactions on Control Systems Technology*, Under revision, 3rd round.
- [25] Y. Tang, Y. Zhang, A. Hasankhani, and J. VanZwieten, "Adaptive super-twisting sliding mode control for ocean current turbine-driven permanent magnet synchronous generator," in *2020 American Control Conference (ACC)*. IEEE, 2020, pp. 211–217.
- [26] Y. Huang, J. Li, M. Shi, H. Zhuang, Y. Tang, X. Zhu, J. VanZwieten, and L. Chérubin, "St-pcnn: Spatio-temporal physics-coupled neural networks for dynamics forecasting," *Scientific Reports (under review)*, 2021.
- [27] J. Su, W. Byeon, J. Kossaifi, F. Huang, J. Kautz, and A. Anandkumar, "Convolutional tensor-train lstm for spatio-temporal learning," *Advances in Neural Information Processing Systems*, vol. 33, pp. 13 714–13 726, 2020.
- [28] C. Zhang, J. Yella, Y. Huang, X. Qian, S. Petrov, A. Rzhetsky, and S. Bom, "Soft sensing transformer: hundreds of sensors are worth a single word," in *2021 IEEE International Conference on Big Data (Big Data)*. IEEE, 2021, pp. 1999–2008.